Composite Structures 242 (2020) 112167

Contents lists available at ScienceDirect

Composite Structures

journal homepage: www.elsevier.com/locate/compstruct

Achieving strong friction lap joints of carbon-fiber reinforced plastic and metals by modifying metal surface structure via laser-processing pretreatment

L.H. Wu[a,b,*], B.L. Xiao[b,*], K. Nagatsuka[a], K. Nakata[a], Z.Y. Ma[b]

[a] Joining and Welding Research Institute, Osaka University, 11-1, Mihogaoka, Ibaraki, Osaka 567-0047, Japan
[b] Shenyang National Laboratory for Materials Science, institute of Metal Research, Chinese Academy of Sciences, 72 Wenhua Road, Shenyang 110016, China

ARTICLE INFO

Keywords:
Friction stir welding
Metal
Carbon-fiber reinforced plastic
Dissimilar joining
Laser processing
Mechanical interlocking

ABSTRACT

Strong dissimilar joints of metals and carbon fiber reinforced plastic (CFRP) are highly demanded for the lightweight design in many fields, which, however, are rather challenging to achieve directly via welding. In this study, 5052 Al alloy and plain carbon steel were first pretreated by a laser-processing method to create rather coarse porous metal surfaces, which were then welded to polyamide 6 based CFRP using friction lap joining. The maximum tensile shear force of the dissimilar joints of CFRP-Al alloy and CFRP-steel achieved 4.9 kN, and 3.9 kN, respectively, and the joint efficiency achieved 78% and 62%, respectively, which were more than three times as those of the CFRP- as-received metal joints. This is the first report on the strengthening of the metal-CFRP friction based joints via the assisting laser treatment technique. The significant improvement of the joint strength could be attributed to a great increase of the mechanical anchors and the chemical bonding area at the metal-CFRP interface.

1. Introduction

As the increasing requirement of lightweight design and excellent performance in the aerospace and automobile industries, the application of plastics and carbon-fiber-reinforced plastics (CFRPs), especially the processable carbon-fiber reinforced thermoplastics (CFRTP) is gradually increasing because of their light weight, excellent corrosion-resistance and superior fatigue properties etc. In many fields, it has been a trend that metals are replaced by plastics based materials. However, because of the unique performance of metals, such as their superior toughness and electrical conductivity, it is impossible that metals are completely replaced by plastic based materials. To combine the advantages of both metals and plastic based materials, the hybrid joining of metals and plastic based materials are highly demanded for the structural applications [1–3].

Conventionally, adhesive bonding and mechanical fastening are the most common joining methods for metals to plastic based materials [4–6]. However, adhesive bonding is usually toxic, susceptible to environmental factors and needs a long time. Besides, for some CFRTP, it is not easy to explore a proper binder, or the binder is rather expensive. For the mechanical fastening, the components suffer from an extra weight increase and stress concentration. Also, the whole carbon fibers throughout the CFRP sheets are generally broken during mechanical fastening. Therefore, in order to solve these problems, novel joining methods, such as laser welding, ultrasonic welding, friction stir welding have recently drawn a lot of attentions for the joining of metals to plastics and CFRPs.

Recently, many researchers [7–10] have reported that laser welding is successfully applied for the joining of the metals to plastics and CFRPs. The joining mechanism was mainly attributed to the chemical and physical bonding, as well as mechanical interlocking effect [7]. Further, the pressure from the expansion of bubbles was reported to be beneficial for the bonding of metals and plastics [7,11]. It was reported that ultrasonic welding could also successfully join metals with plastics and their CFRPs, and the tensile shear strength (TSS) of the joints could achieve 58 MPa [12–14]. The joining mechanism was mainly related to mechanical interlocking effect and Van der force [12–14]. However, both laser and ultrasonic welding have some shortcomings. For the laser welding, there are too many bubbles coming from the thermal decomposition of plastics remaining in the joint, which will deteriorate the joint properties. Also, the laser joint quality is easily affected by the optic characteristics of the welded materials. For example, for the joint of CFRP to the metals with low laser absorption efficiency such as Cu and Mg, a high quality is very difficult to achieve. For the ultrasonic

* Corresponding authors at: Institute of Metal Research, Chinese Academy of Sciences, 72 Wenhua Road, Shenyang 110016, China (L.H. Wu).
E-mail addresses: lhwu@imr.ac.cn (L.H. Wu), blxiao@imr.ac.cn (B.L. Xiao).

https://doi.org/10.1016/j.compstruct.2020.112167
Received 19 September 2019; Received in revised form 3 February 2020; Accepted 10 March 2020
Available online 14 March 2020
0263-8223/

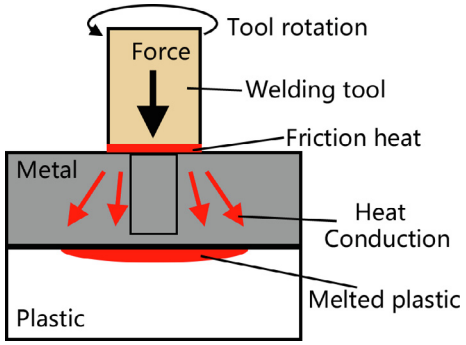

Fig. 1. Schematic of friction stir lap welding of plastics and metals.

welding, there exists dimension limiting for the welding components, which limits its wide application. Besides, both of them are now still in a developing stage, some basic knowledge such as the joining mechanism and the relationship of process-structure-property is still unknown, and the joining efficiency is still needed to be enhanced. Thus, other joining methods are also highly needed to explore the feasibility of high-quality joints.

Friction stir welding (FSW), invented in 1991, has been widely used in Al, Mg, Ti etc [15–19], and recently applied into the hybrid joining of metals and plastic based materials [20–24]. The typical principle of FSW for lap joining of metals and plastic based materials is shown in Fig. 1. A rapid temperature rise in metals is caused by the friction between the rotated welding tool and workpieces, which is conducted to the plastic below, and makes it melt. Then, the metal is pushed into the melting plastic under the pressure of welding tool, and finally the joining of the metal and the plastic is successfully achieved. Therefore, the FSW of the metal and plastic based material shows several advantages as follows. 1. No dimension is limited and 3D welding is possible. 2. Heat input is controllable in a wide range, avoiding too much plastic decomposition. 3. The thermomechanical process during FSW is controllable, and the bubbles caused by thermal decomposition can be expelled out of the joint. 4. No limiting from the optical characteristics of the workpieces. Thus, it is a promising joining method for metals and plastic based materials.

Recently, many researchers [2,20–26,28–31] have found that FSW can successfully join metals with plastics and their CFRPs. For example, Goushegir et al [2] found that friction stir spot welding is feasible for the successful joining of AA2024 Al alloy with poly(phenylene sulfide) (PPS) based CFRP. Besides, Huang et al. [28,29] reported that it was successfully achieved for the joining of Al alloy to polyether-ether-ketone (PEEK) and its CFRP via FSW with a special stationary shoulder and pin design, and the TSS could achieve 33 MPa. However, the carbon fibers were severely destroyed by the stirring effect, which would affect the joint property. In order to avoid or reduce the destroying of carbon fibers as much as possible, Nakata and his coworkers [22,23,25] developed a new varied FSW method, i.e. FSW with a welding tool without a pin, called as friction lap welding (FLJ) to join metals to plastics and CFRPs. They found that FLJ could directly join Mg, Al, Cu, steel to polyamide 6 (PA6) based CFRP with a relatively low degree of carbon fiber damage [20,22,27,30]. However, the metal-CFRP FLJ joints have been reported to show a low TSS of only 4–13 MPa (< 3 kN for 15 mm wide weld) [20,22–23,30].

As we know, during welding, the joining of metals and plastic based materials can be generally achieved by chemical bond, hydrogen bond, Van der bond, and/or mechanical interlocking effect at the joint interface. For the metal-CFRTP joint directly by FLJ, the main joining mechanism was attributed to the chemical bond or hydrogen bond at the interface, but the bonding area was relatively small [20], and the mechanical interlocking effect was very little as well [20]. Therefore, the joint strength was relatively low. In order to avoid the damage of the carbon fiber as much as possible, and improve the joint strength at the same time, to largely enhance the chemical bond area and/or the mechanical interlocking effect at the interface during FLJ is a good choice.

More recently, Lambiase et al [32–34] utilized a variant FSW process, called as friction assisted joining (FAJ) to join metals to plastics. The principle of FAJ is very similar to FLJ, but the difference is that FAJ has been mainly used as a spot joining [32–34], while FLJ has been mainly used as a line joining [20–23]. Lambiase et al [32–34] first utilized laser processing pretreatment to modify the surface structures of Al and Ti alloys, and then used FAJ to successfully join these laser pretreated metals with plastics including PEEK and polyvinyl chloride (PVC). The maximum shear strength of the PEEK-Ti joint and the PEEK-Al alloy joint were achieved 37.3 MPa and 47 MPa, respectively. It suggested that the laser processing pretreatment on the metal surface was benefit for largely enhancing the metal-plastic joint strength, and the large increase of the mechanical anchors contributed a lot to the joint strength increase. However, the metal-plastic joining could not represent the typical welding condition of metals to CFRPs, since carbon fibers with high thermal conductivity largely affect the heat transfer, but the plastics do not contain carbon fibers, which shows a poor thermal conductivity. Besides, the flowing and solidification characteristics of the plastic matrix in CFRPs are probably different from the pure plastics. Moreover, all these studies on the laser processing combining with FAJ only focused on the spot joining, and thus the joined component was limited. Furthermore, most studies have mainly focused on the joining of plastics (and CFRPs) to Al alloys, but limited reports were made on steel-CFRP FLJ joints, and the strength of the CFRP-steel FLJ joint was relatively low [30,35]. So far, seldom studies have been reported to strengthen metal-CFRP FLJ joints by extra surface pretreatment methods, such as the laser processing pretreatment.

Therefore, in this study, a laser processing pretreatment was made in the surface of the Al alloy and steel sheets, and the metal flat surfaces were modified into coarse porous surfaces. FLJ was applied to the joining of PA6 based CFRP to the laser processed Al alloy and steel. This study aims to explore the feasibility of largely enhancing the strength of the metal-CFRP hybrid joints by modifying the metal surface structure via laser processing pretreatment.

2. Experimental procedure

The as-received materials were 3-mm-thick CFRTP with PA6 matrix ($[NH(CH_2)_5CO]_n$ with 20 wt% carbon fiber addition) sheets, 2-mm-thick 5052 Al alloy and plain carbon steel (SPCC) sheets. The diameter and length of the carbon fibers were 10 μm and ~500 μm, respectively, and about more details on the CFRTP, please refer to the previous work [23]. Before FLJ, CFRTP sheets were dry-ground with #80 and #800 emery paper. For the metal 5052 Al alloy and SPCC plates, the surfaces were processed by laser-irradiation with three different powers, producing the coarse surfaces with lots of pores with different depth, and the schematic of laser processing pretreatment on the metal surface is shown in Fig. 2. The samples of the metal surfaces treated by laser-

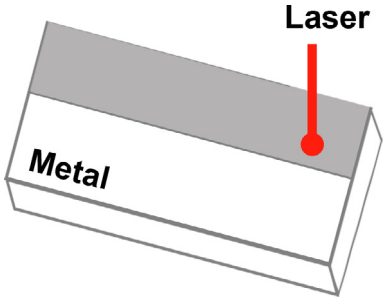

Fig. 2. Schematic of laser processing pretreatment on metal surface.

irradiation were provided by Daicel Polymer Ltd. When the laser power was weak, medium, and strong, the 5052 Al and SPCC samples by laser processing treatment were marked as 1#, 2# and 3#, respectively. In the previous studies [23,35,36], the 5052 Al with silane coupling pretreatment was joined to PA6 based CFRTP using the 1000–2000 rpm, 100–1600 mm/min and the optimum parameter of 5052 Al-CFRTP was 2000 rpm, 400 mm/min. Besides, 2000 rpm, 400 mm/min and 2000 rpm, 1200 mm/min were also tried to explore the feasibility of the joining of the laser processed 5052 Al to CFRTP. It was also found that 2000 rpm, 400 mm/min was the optimum parameter. In addition, as-received SPCC was joined to PA6 and PA6 based CFRTP using the parameters of 1000 rpm, 100–800 mm/min, and the optimum parameter was 1000 rpm, 600 mm/min [35]. Based on the similar FLJ condition, 2000 rpm, 400 rpm and 1000 rpm, 600 mm/min were selected as the FLJ parameters for the laser processed 5052 Al-CFRTP and SPCC-CFRTP joints in this study. A tool plunge depth of 0.9 mm, a tilt angle of 3 degree, and the lap width of 30 mm was used via a SKD tool steel and WC-Co tool with a shoulder diameter of 15 mm without a pin for CFRTP-Al alloy and CFRTP-SPCC joining, respectively. In order to avoid the damage of carbon fiber, the tool was controlled to plunge only into the metal but not contact the CFRP. The penetration of the tool shoulder into the metals could not only generate friction heat between the tool and the workpiece, but also provide enough pressure, so as to make the successful joining of the metals to CFRPs.

For the cross-sectional specimens for microstructural observation, the specimens were cut perpendicular to the joining direction, mounted in epoxy resin, and ground and polished with silica solution. The microstructural observation of these specimens was then performed via optical microscopy (OM) and scan electron microscopy (SEM). To test the tensile shear strength, specimens were cut perpendicular to the joining direction with a width of 15 mm and carried out in a regular tensile test machine at the crosshead speed of 0.5 mm/min. For each joining condition, three tensile specimens were tested. The fracture surfaces of the tensile shear specimens were observed using SEM.

3. Results and discussion

3.1. The surface morphologies of the laser processed Al alloy and steel

The surface morphologies of the laser processed 5052 Al alloy base materials (BMs) are shown in Fig. 3. It is obvious that the 5052 Al alloy sheets exhibited rough and porous surfaces after the laser processing pretreatment. For the sample 1#, the size of the pores was relatively small, but as the laser power increased, the size of the long and narrow shaped pores increased. The cross-sectional microstructures of the laser processed Al alloy BM are shown in Fig. 4. The laser processed beads showed irregular shapes with some cracks. Besides, in the different positions of the beads, the width and depth were different. As the laser power increased from 1# to 3#, the depth and width of the laser processed structure increased, with the depth from ~120 μm to ~240 μm. The width of the pores for the sample 1# was about 20–30 μm. But for the sample 2# and 3#, the width of the pores was much larger, some even achieved 100 μm or more. For the laser processed SPCC BM, a rough and porous surface also exhibited, but the pores showed a relatively regular, parallel-arranged long and narrow shape. Their roughness, the pore size and the pore depth showed the same trend as that of the 5052 Al alloy with the laser power increasing, as shown in Figs. 5 and 6. The depth of the laser processed structure increased from ~105 μm to ~150 μm from 1# to 3#. The width of the laser processed beads was ~38, ~43 and ~44 μm, respectively.

3.2. The feasibility of the joining of laser processed metals to CFRPs

Fig. 7 shows the macrostructural surface morphologies of the joints of the CFRP to the laser processed 5052 Al alloy and SPCC. FLJ could join the CFRP with the laser processed 5052 Al and SPCC alloy well, and the joints could not be separated apart by hand forces. The tensile shear force (TSF) of the joints (Figs. 8 and 9) further confirmed that the hybrid joining was strong. For the joints of the laser processed Al alloy and CFRTP, the maximum TSF reached about 4.9 kN (21.8 MPa for the nominal TSS) for the 1# sample, which was 78% of the CFRTP BM. That is to say, the joint efficiency for the laser processed Al alloy and CFRTP achieved 78%. As the depth of laser processed beads increased, the TSF decreased. Compared to the FLJ joint of CFRP with the 5052Al with no treatment or with being ground under water [23], the TSF increased by more than twice and once, respectively (Fig. 8). It suggested that the laser processing pretreatment on the 5052 Al alloy sheet was an effective way to largely enhance the joint strength. Besides, it was found that the joints for the CFRTP to the laser treated Al alloy usually fractured at both the CFRTP BM and the re-solidified CFRTP near the interface, while it fractured along the Al-CFRTP interface for the joints with the as-received or wet-ground surface. It means that the fracture mode changed after the metal surface was pretreated by laser processing.

For the joints of the laser processed SPCC and CFRP, the TSF of the joints all exceeded 3.5 kN (Fig. 9). As the size of the laser processed beads increased, the joint TSF just slightly decreased, and the maximum TSF reached about 3.9 kN for the 1# sample (the maximum normal TSS was 17.3 MPa), and the joint efficiency was 62%. Besides, the joint strength after the laser processing pretreatment was more than three times as those of the joint for SPCC with an original or wet-ground surface state. It suggested that the laser processing pretreatment on the surface of metals was a very effective way to enhance the joint strength by even more than twice.

3.3. Microstructure and fracture morphology of the laser processed Al alloy to the CFRP

The cross-sectional macrostructures of the joints of CFRTP and the laser processed 5052 Al alloy are shown in Fig. 10. It is obvious that the laser processed porous surfaces have been filled in the melted plastic of CFRP (white band), which thus formed a large number of mechanical anchors at the CFRTP-5052 Al interface. The magnified microstructures of the interface in the joint are shown in Fig. 11a and b, which further confirmed the mechanical interlocking effect of the hybrid joints. For comparison, the interface of the FLJ joint of the wet-ground 5052 Al

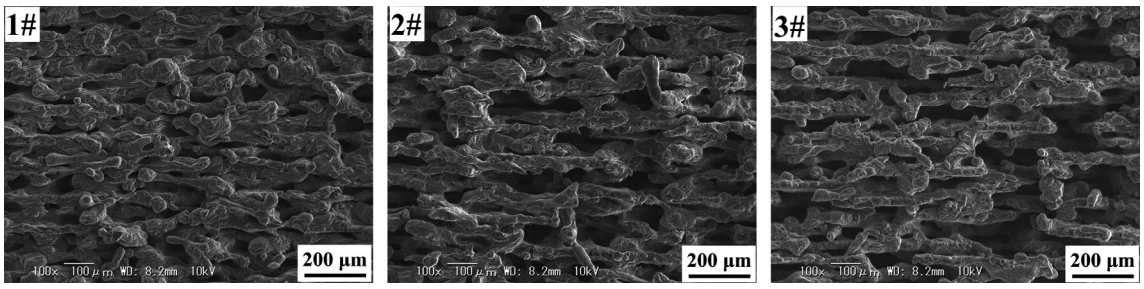

Fig. 3. Surface morphologies of laser-processed 5052 Al alloy.

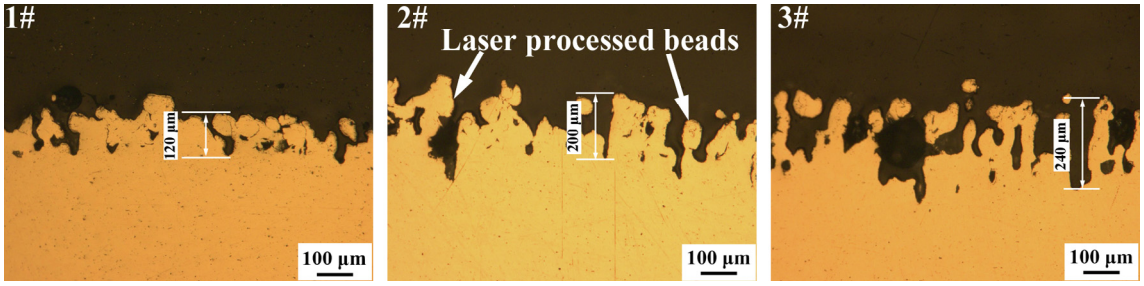

Fig. 4. Cross-sectional microstructures of laser processed 5052 Al alloy.

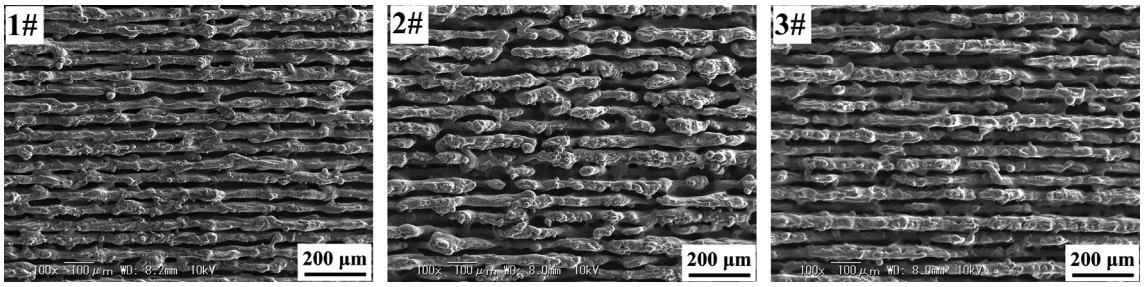

Fig. 5. Surface microstructures of laser processed SPCC steel.

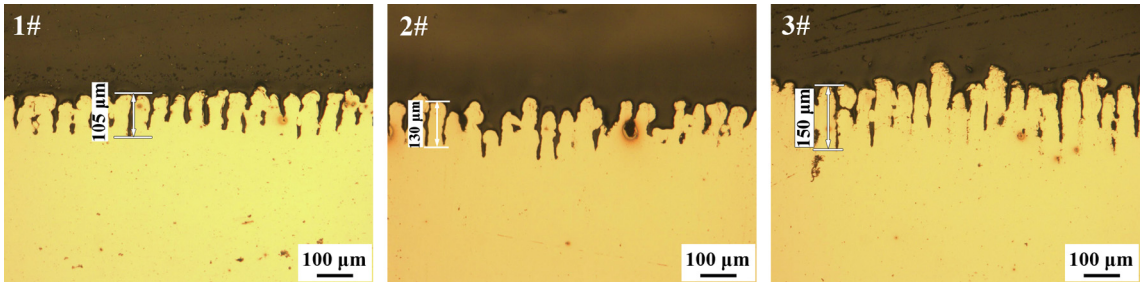

Fig. 6. Cross-sectional microstructures of laser processed SPCC steel.

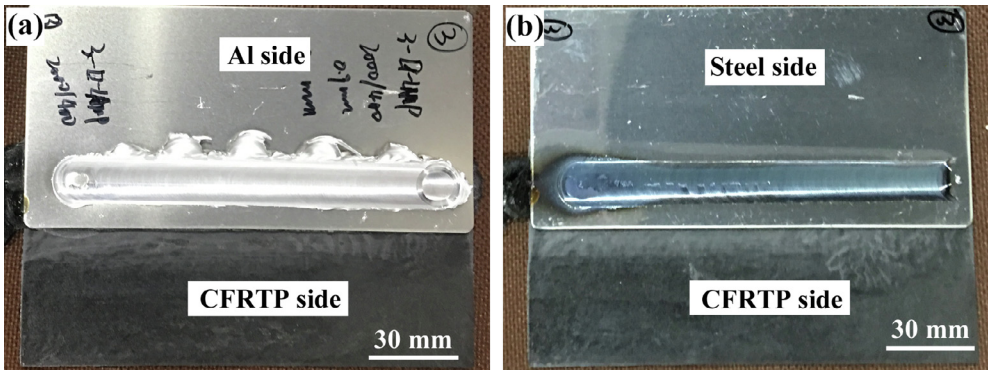

Fig. 7. Surface morphologies of friction lap joints of CFRTP to laser-processed: (a) 5052 Al alloy and (b) SPCC steel.

alloy and CFRTP is also shown in Fig. 11c. The mechanical anchor was hardly observed at the Al-CFRTP interface of the FLJ joint without laser surface treatment [23,37]. Therefore, one reason for the large increase of the joint strength via the laser processing was probably attributed to the large increase of the mechanical anchors at the interface. Besides, it could be also observed that the tight bonding with no crack was achieved between the Al alloy and CFRTP (Fig. 11b), which might be attributed to the form of chemical bond of the Al alloy and CFRTP.

It was reported that the main joining mechanism of metals and the plastics with a carbonyl function group (C═O, such as PA) was attributed to the chemical bond of C-O-Al at the interface which was formed by the reaction result of metal oxide on the metal surface and the carbonyl group of the plastics [38]. Therefore, in this study, the chemical bond of C-O-Al might have been formed, and the tight bonding at the interface might be the result of the formation of the C-O-Al chemical bond. Compared the interface for Al-CFRTP joint with and without laser surface treatment (Fig. 11a and c) [37], it is obvious that the porous structure by the laser processing pretreatment probably largely enhanced the area for the chemical bonding, thereby enhancing the interface strength. Thus, the Al-CFRTP interface was probably largely strengthened by the increased mechanical anchors and chemical bond area, which thus largely enhanced the joint strength.

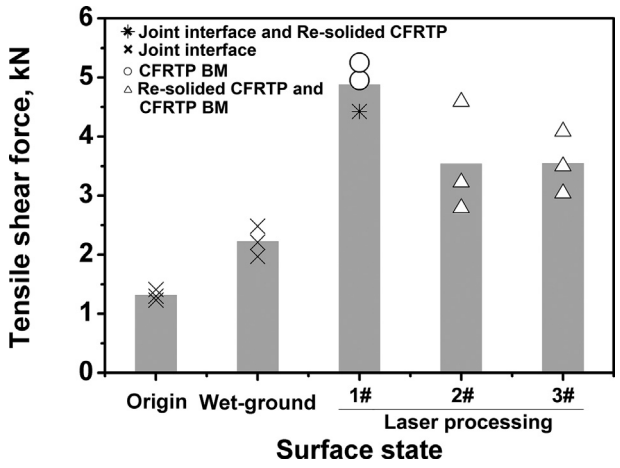

Fig. 8. Variation of tensile shear force with the surface treatment condition for the FLJ joints of 5052 Al alloy to CFRTP. The data for the original and wet-ground statement was referred from [23].

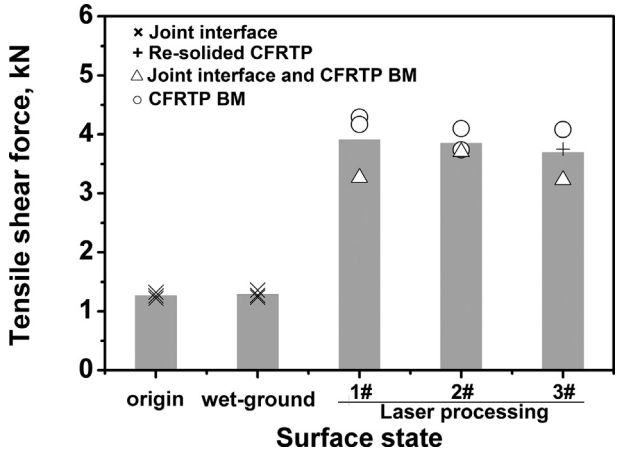

Fig. 9. Variation of tensile shear force with surface treatment condition for FLJ joints of SPCC steel to CFRTP.

Further observation by optical microscopy shows that a large number of bubbles were observed near the interface of CFRTP and Al alloy. However, for different joints from 1# to 3#, the bubbles at the re-solidified CFRTP side near the interface were totally different (Fig. 12). As the laser power increased, the bubbles near the interface increased. For the sample 1#, bubbles were hardly observed in the laser processed beads. But the bubbles were even observed within the beads in 2# and 3#, especially in the beads of 3#, some beads was completely full of bubbles. As we know, for the same FSW parameter for the same material, the heat input should be almost the same. Therefore, the formation of bubbles from the thermal decomposition of PA6 was almost the same for the joints 1# to 3#.

The different bubbles in different joints were likely because that the different depth and width of the pores affected the flowing of the bubbles. For the large depth and width of the laser beads, the depth of the beads was too large that the air could not be expelled out completely, or the width of the laser processed pores was too large that bubbles originated from the thermal decomposition were flown into these pores of the laser processed beads. As a result, the distribution of bubble was different. As the bead depth increased, the size and fraction of bubbles increased. The bubbles were usually the weak region of the joint during tension, acting as the fracture pass sites. Therefore, these bubbles in the beads or near the interface likely deteriorated the joint strength, thereby reducing the TSF.

In order to further explain the fracture reason, the fraction surfaces on the Al side were observed, and the typical fracture surfaces for the joints 1# and 3# are shown in Fig. 13. For the Al fracture surface of the joint 1#, a large amount of CFRTP was stuck on the Al alloy sheet with seldom bubbles (Fig. 13b). It indicated that the joint fractured along the re-solidified plastic near the interface, and the bubbles might seldom affect the fracture for the 1# sample. But for the 2# and 3# samples, there were a large amount of bubbles at the fracture surface (Fig. 13d), which suggested that the bubbles was probably the site for the fracture pass.

Generally speaking, there are three weak regions, i.e. the interface, bubble and the re-solidified plastic near the interface [20]. It means that strengthening the interface, reducing the bubbles, especially the large-sized bubbles and reducing the thermal decomposition of plastic are the main methods to enhance the joint strength. In this study, for the laser processed metal, a large number of mechanical anchors due to the plastic trapped into the metal pores were formed after FLJ. Also, the area of the chemical bond increased due to the laser processed porous surface. Therefore, the interface has been largely strengthened by the great increase of the mechanical anchors and the area of the chemical bonds. For all the three laser processed surfaces, the same parameter means that the degradation of PA6 was almost the same. As the depth of the laser processed structures increased, the fraction and size of bubbles increased (Fig. 12). Thus, Compared to the sample 1#, the bubbles might become the weakest region and thus largely deteriorate the joint strength for samples 2# and 3#.

3.4. Microstructure and fracture morphology of the laser processed steel to the CFRP

The cross-sectional macrostructures of the laser processed SPCC – CFRTP joints were observed, as shown in Fig. 14. It is obvious that not all the lapped area in the overlapped zone was joined, which was different from that of Al alloy where all the lapped zone was joined well (Fig. 10). It might be attributed to two aspects. First, Al alloys have a better thermal conductivity than the SPCC, so that the whole Al sheet could be heated quickly, and the melting CFRTP was flown across the lapped zone. But for the SPCC, due to the lower thermal conductivity of steel, the edge of the steel sheet could be not heated immediately and some CFRTPs could not flow into the edge, and thus at this region, effective joining could not be achieved. Second, the Al alloy shows a lower strength than the SPCC, and thus the Al alloy could deform more easily to form an almost flat shape conforming to the tool shoulder (Fig. 10). While the SPCC, having higher flow stress, deformed into a

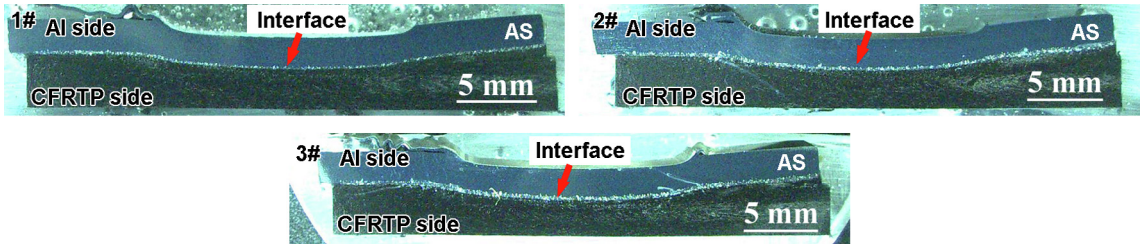

Fig. 10. Cross-sectional macrostructures of friction lap joints of laser-processed 5052 Al alloy to CFRTP.

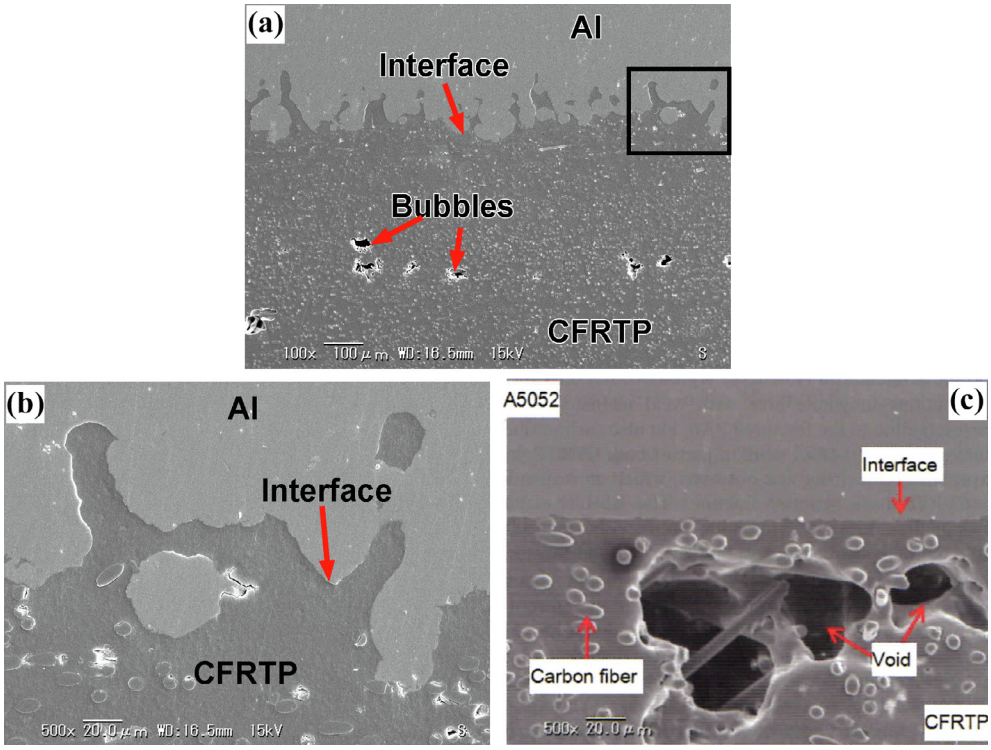

Fig. 11. Typical SEM images of 5052 Al-CFRTP friction lap joints with (a) (b) laser-processed treatment in this study, and (c) Al alloy surface ground in water cited from the reference [31].

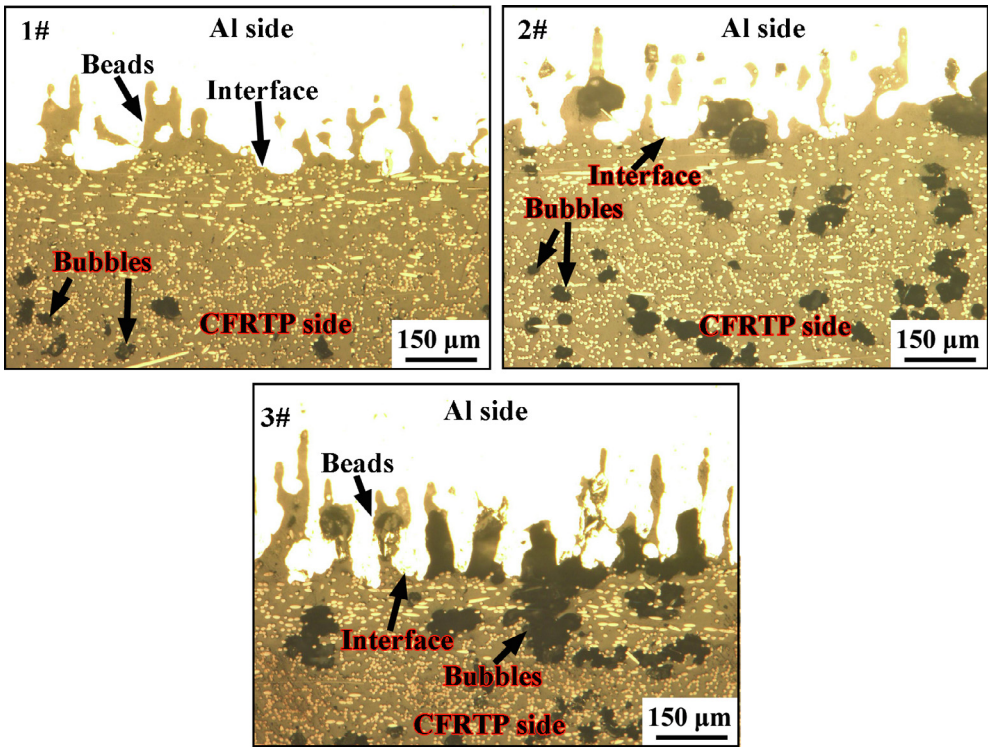

Fig. 12. OM images of friction lap joints of laser-processed 5052 Al alloy to CFRTP.

bow-shape (Fig. 14), which in turn reduced the interface area with the CFRTP.

For the magnified microstructural images, the mechanical anchors were observed at the typical CFRTP-SPCC interface (Figs. 15 and 16). Within the CFRTP near the interface, a large number of bubbles formed by the thermal decomposition of PA6 were observed. Besides, the tight bonding without cracks was observed at the PA6-SPCC interface. Also, within the laser processed pores, almost all the pores throughout the depth were filled entirely in the PA6, and the PA6 flown into the pores was also bonded tightly with the SPCC. It was reported that it was easy to form a chemical bond between the C═O functional group and metal oxide on the metal surface [38]. Thus, it could be inferred that Fe might

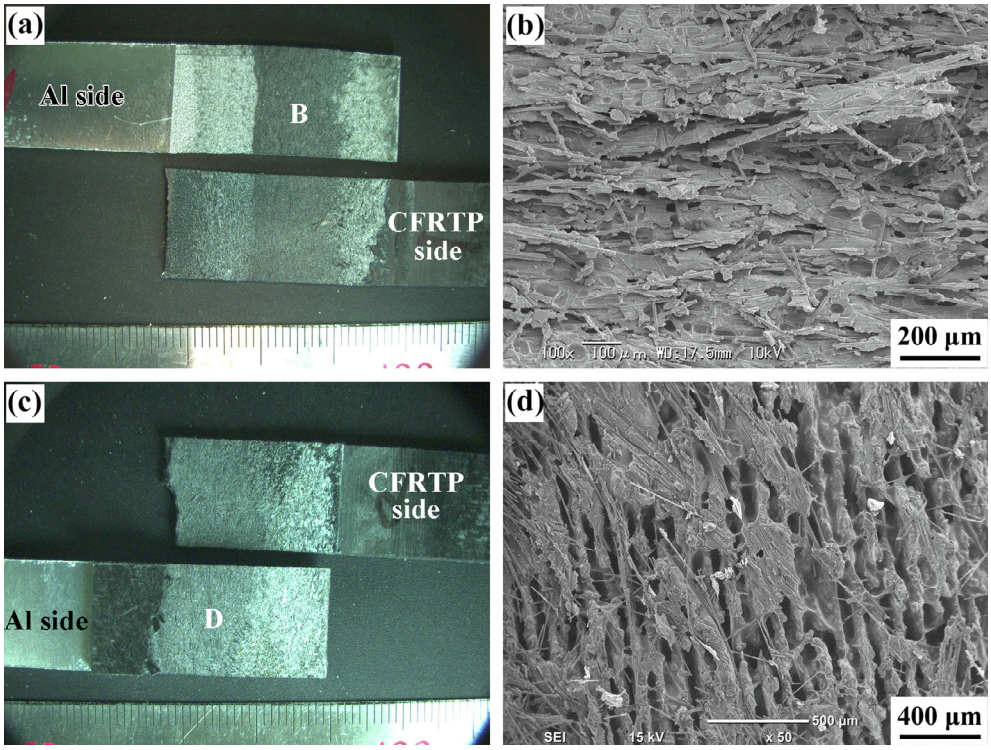

Fig. 13. Typical fracture surfaces of 5052 Al-CFRTP friction lap joints with (a) joint 1# and (b) magnified SEM image in area B in (a), (c) joint 3#, and (d) magnified SEM image in area D in (c).

have also formed a chemical bond with the CFRTP at the interface similar to the Al-CFRTP joints. Moreover, the laser processed pores were mainly full of PA6 with very few carbon fibers because of the easier mobility of melted PA6 than the carbon fibers. Besides, seldom bubbles were observed in the laser beads of the SPCC, which might be because of the narrow and deep pores for the SPCC, it was difficult for the bubbles to flow into the pores. For all the three parameters, there were too many bubbles and some even joined together into large bubbles (> 40 μm) at the interface, which would deteriorate the joint strength largely.

The fracture surfaces of the SPCC-CFRTP joints are shown in Fig. 17. It is clear that the bubbles were one of the fracture pass sites (Fig. 17a). Also, the joint fractured along the interface with some PA6 stuck to the beads, indicating that SPCC probably formed a tight bond with CFRTP, which agrees with the microstructural observation in Fig. 15. The magnified microstructure on the fractured CFRTP surface is shown in Fig. 17d. It is obvious that a shear feature exhibited in the CFRTP but there was no shear feature within the bubbles. It suggested that the bubbles usually did not bear the load, thereby deteriorating the joint strength.

According to the fracture surface morphologies of both CFRTP to Al alloy and steel joints, the schematic diagram of fracture pass is shown in Fig. 18. Bubbles were one of the most important fracture pass. Due to the mechanical interlocking effect and the chemical bonding at the interface, the CFRTP and laser processed metals could join very well at the interface, while the re-solidified polymer or bubbles largely affected the joint strength. Therefore, the region at the re-solidified CFRTP layer near the interface and bubbles became the weakest area, thereby becoming the fracture pass.

3.5. The main advantages and further investigation of FLJ assisted by the laser processing pretreatment

As was mentioned above, maximum TSFs of 4.9 kN and 3.9 kN of Al alloy-CFRP and SPCC-CFRP joints were achieved by FLJ assisted by the laser processing pretreatment. Generally, to indicate which welding parameters or methods were of more advantages, the joint strength for the similar welding materials with similar joining methods was used for comparison. However, to our best knowledge, there has been no available data in the literature on the mechanical property of SPCC-CFRP friction based joints, and limited data on that of Al alloy-CFRP (PA6 based) FLJ joints [23]. In addition, the practical joint TSS is difficult to be calculated since the real joining area is difficult to be measured. Thus, in order to compare the bearing capacity of the metal-CFRP friction based lap joints, the maximum TSF and normal TSS for different metal-CFRP friction based lap joints in the literatures and this study are attempted for comparison (as many literatures [1–3,39–40] has adopted), as listed in Table 1.

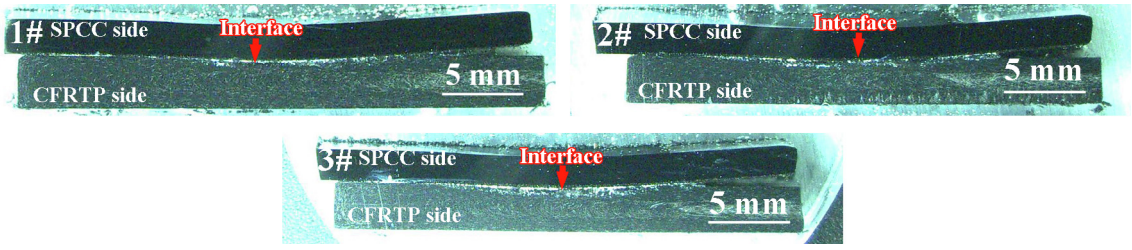

Fig. 14. Cross-sectional macrostructures of friction lap joints of laser-processed SPCC steel to CFRTP.

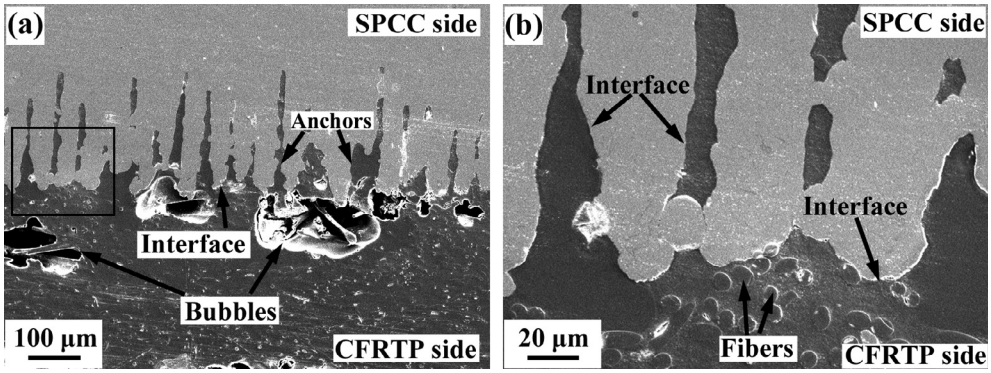

Fig. 15. SEM images of cross sections of SPCC steel-CFRP joint showing: (a) bubbles and (b) interface joining.

It was found that for all the metal-CFRP FLJ joints, the TSF and normal TSS of no more than 3.6 kN and 16 MPa was obtained directly by FLJ, respectively (No. 3–6 in Table 1 [20,21,23,30]). While when a laser processing pretreatment was made on the metal surface in this study, both the TSF and TSS of the metal-CFRP joints were improved (Nos. 1–2 in Table 1). The large joint strength increase should be mainly attributed to two aspects. First, for the metal-CFRP joints directly by FLJ, mechanical anchors were hardly observed [20,21,23,30], while after laser processing pretreatment, a mechanical interlocking effect at the metal-CFRP interface was largely enhanced by the deep porous structures, which improved the joint strength. Second, after laser processing, the porous structure surface largely increased the contact area for the metals to the CFRPs, which thus increased the bonding area, thereby improving the joint strength. Therefore, using the laser processing pretreatment on the metal surface was an effective way to largely enhance the strength of the metal-CFRP FLJ joints.

It was also found that a large TSS of more than 22 MPa could be achieved by friction based joining using a tool with an independent pin and shoulder or using a pre-threaded hole (No. 7–13 in Table 1 [2,3,24,29,31,39,40]). It might be the result that compared to the conventional welding tool, the novel tool including the independent pin and shoulder could better control the heat time, pressure and cooling process. Or the mechanical interlocking effect could be increased via using a pre-threaded hole. Thus, it might be a good way to enhance the friction based joint strength using a tool with independent pin and shoulder or using a pre-threaded hole. However, at present, this method is still mainly limited for the spot welding. Therefore, the welded component is largely limited.

More importantly, although a high normal joint TSS was achieved by these methods, the joint TSF was not large (< 3.6 kN, Table 1). As we know, in practical engineering application, the TSF rather than the normal TSS for lap welding represents the joint bearing capacity. For example, although some joints show a high normal TSS, if the joining area is small, the joint still shows a poor bearing capacity. Take the Nos.7 and 8 in Table 1 [29,31] for example, the load for the lap joints was only ~1.56 and ~0.35 kN, respectively, even if the normal TSS was even as high as 33 and 28 MPa, respectively. Therefore, these kinds of joints might be still limited for the engineering application even if there is a high normal TSS exhibited in the joint.

Actually, in many cases, the real joint TSS was totally different from

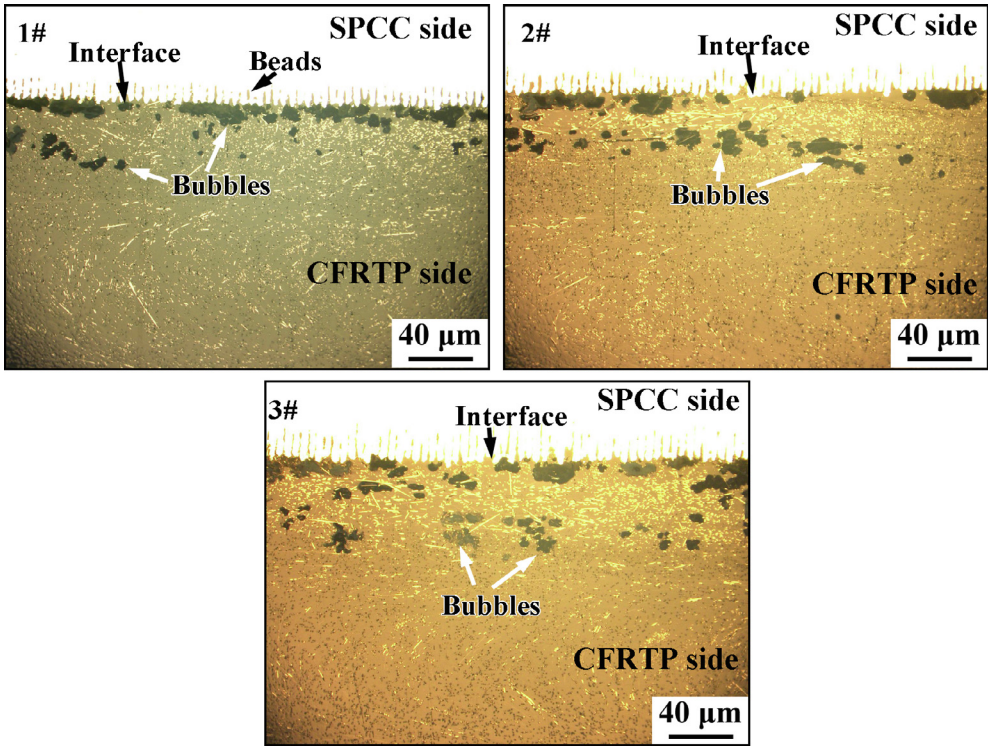

Fig. 16. OM images of friction lap joints of laser-processed SPCC steel to CFRTP.

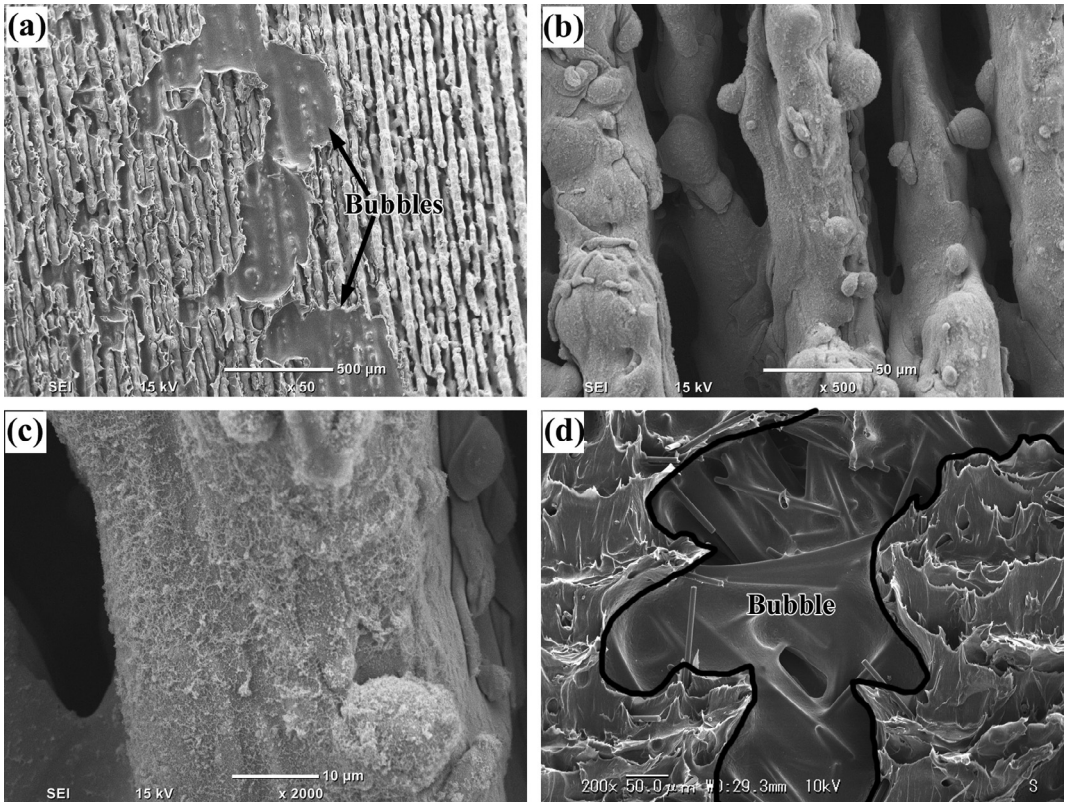

Fig. 17. Typical fracture surfaces on SPCC side of SPCC steel-CFRTP friction lap joints: (a) whole fracture surface, (b) magnified SEM image of laser beads in (a), (c) magnified SEM image of (b), and (d) SEM image of the fractured CFRTP side.

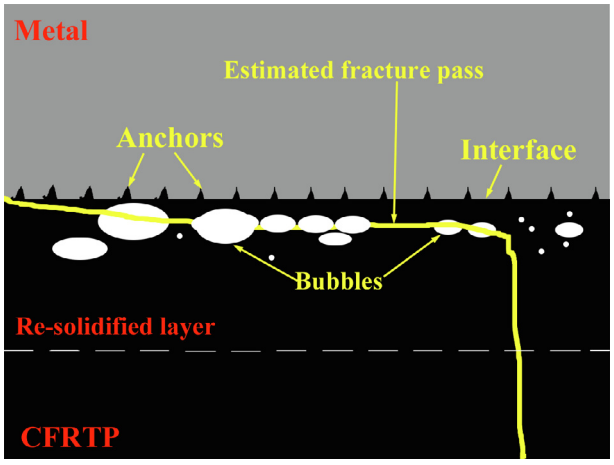

Fig. 18. Schematic of fracture pass of metal-CFRTP FLJ joints.

the normal TSS, because the real joining area might be totally different from the normal welding area, and the normal TSS for the lap joint could not well reflect the joint bearing capacity. For example, in No. 9–12 in Table 1 [2–3,39–40], although the normal welding area of these joints was the same, i.e. the tool (sleeve) area, 63.6 mm^2, the real joining area was totally different for these joints (differed from 275 to 590 mm^2). Therefore, the normal TSS for these joints could not be the index to reflect the joint bearing capacity since it might be enlarged artificially.

Therefore, from this aspect, the TSF is more suitable to be the index for comparing the bearing capacity for the lap joints than the TSS. Unfortunately, the tensile specimen width also affects the joint TSF, especially for the FLJ joints. Therefore, it might be better to indicate the joint bearing capacity with the joint TSF, but assisted by the TSS. In this study, both the TSF and TSS of the Al-CFRP and steel-CFRP joints was relatively large (Table 1), which suggested that the joints in this study had a good bearing capacity. Therefore, the laser processing surface pretreatment on the Al alloy combining with FLJ is good way to largely enhance the metal-plastic joint strength.

Therefore, FLJ assisted by the laser processing pretreatment in this study has exhibited some advantages. First, the welding components could not be limited by the welding dimension. Second, the tool design in this study is very simple and the cost is low, which is more suitable for the engineering application compared to the complex tool design. Third, since the large mechanical anchors could form once the melted plastic penetrated into the pores of the laser processed metals, it is suitable for different metals and different plastic based CFRPs, including non-polar plastics, like PP based CFRP, which has been proved by our studies, and it has been reported in [41]. In fact, there are lots of surface pretreatment methods, such as sand blasting, surface anodizing, laser processing etc. Assisted by these surface pretreatment methods, the joint strength could be improved [3,40]. Among these surface pretreatment methods, the laser processing method is a good surface pretreatment to well control the surface roughness, the depth and width of the pores in a large range. In the future, the combination of FLJ with the laser processing surface treatment might be the developing direction.

At present, the welding of metals to CFRPs assisted by the laser processing pretreatment is still in a developing stage. To promote the developing of this method in the future, some suggestions are attempted to be proposed as follows. First, based on the thermal and flowing characteristics for different materials, using a special-designed tool, clamp and pre-treated hole etc. for FLJ assisted by the laser processing method or other surface pretreatment methods might be an important improved method to enhance the metal-CFRP joint strength. Second, it was found that the bubbles in the joints were still a key factor influencing the joint quality in this study, and especially for the laser

Table 1
Maximum tensile shear force and strength of the friction based joints of CFRP to Al alloys and steel from different researchers.

No.	Method (materials)	Max TSF, kN	Max normal TSS, MPa (% of plastic BM)	Normal welding area, mm^2	Remark	Ref.
1	FLJ (5052Al-CF/PA6)	4.9	21.3	15 × 15	5052 Al: laser processing, porous; Tool Φ15mm without pin; part of CFRP BM fracture	This study
2	FLJ (SPCC steel-CF/PA6)	3.9	17.3	15 × 15	SPCC steel: laser processing, porous; Tool Φ15mm without pin; part of CFRP BM fracture	This study
3	FLJ (5052 Al -CF/PA6)	2.9	12.9	15 × 15	5052 Al alloy: ground underwater Tool Φ15mm; Interface and part of CFRP fracture	[23]
4	FLJ (304 stainless steel-CF/PA6)	2.5	11.1	15 × 15	Tool Φ15mm; Interface and part of CFRP fracture	[30]
5	FLJ (Cu-CF/PA6)	2.3	10.2	15 × 15	Tool Φ15mm without pin, Interface fracture	[20]
6	FLJ (Cu-CF/PA6))	3.54	15.7	15 × 15	Tool Φ15mm without pin, Tool offsetting, BM fracture	[21]
7	FSLW* (2060 Al-CF/PEEK)	~1.56	33	~47.4	Stationary shoulder, rotational shoulder and tapered thread pin with the triple facets; Tool Φ8mm; Interface fracture	[29]
8	THFSW* (5052 Al-CF/PP)	0.35	~28	π × 2^2	5052 Al alloy: Pre-threaded hole Φ4 mm; Tool Φ20mm without pin; Interface fracture	[31]
9	FSpJ* (2024 Al-CF/PPS)	2.69	43	π × 4.5^2	2024 Al alloy: alclad, sand blasting; Tool Φ9mm with independent pin; Interface fracture; Joining area: ~275 mm^2	[2]
10	FSpJ (2024 Al-CF/PPS)	2.31	~36	π × 4.5^2	2024 Al alloy: sand blasting; Tool Φ9mm with independent pin Φ6mm; Interface fracture; Joining area: ~470 mm^2	[3]
11	FSpJ (6181 Al-CF/PPS)	3.52	~55.4	π × 4.5^2	Double lap joint; Tool Φ9mm with independent pin; Interface fracture; Joining area: greater than 350 mm^2	[39]
12	FSpJ (2024 Al-CF/PPS)	3.07	~48	π × 4.5^2	2024 Al alloy and CFRP: sand blasting; PPS film Interlayer addition; Tool Φ9mm with independent pin; Interface fracture; Joining area: ~590 mm^2	[40]
13	FSpJ (AZ 31 Mg-CF/PPS)	~1.4	~22	π × 4.5^2	Tool Φ9mm with independent pin Φ6mm; Interface fracture	[24]

* FSLW: Friction stir lap welding; THFSW: Threaded hole friction spot welding; FSpJ: Friction spot joining; PP: Polypropylene.

processed Al alloy with too large and deep pores (3# sample in Fig. 2), a large number of bubbles were found in the joints. Therefore, how to effectively control the bubbles in the joints and to optimize the morphology, depth, distance, size etc. of the laser processed pores will be an important direction for further investigation of the metal-CFRP joint in the future.

Third, it was found that the previous reports focused on the friction based joining of Al alloys to PA6, PEEK and PPS based CFRPs [23,29,39,40], but the friction based joining of other plastics and their CFRPs to metals was reported very limitedly, and the strength of these joints was relatively small. Thus, to promote the industry application of metal-CFRP joints, to develop the friction based joining of different kinds of metals and CFRPs and enhancing the joint quality are highly needed. Also, some properties such as corrosion properties, fatigue properties and some other properties besides the static tensile shear properties of the metal-CFRP joints are highly needed to be studied in the future.

4. Conclusions

In this study, strong lap joints of CFRTP to Al alloy and steel were successfully achieved for the first time by modifying the metal surface structure via the laser processing pretreatment, and the following conclusions were made.

1. The maximum TSF of the joint of CFRTP to the laser processed 5052 Al and SPCC achieved 4.9 kN and 3.9 kN respectively, more than three times as those of the metal-CFRTP joints without surface pretreatment (< 1.5 kN).
2. The large enhancement of the joint strength via the laser processing pretreatment was attributed to the large increase of the mechanical anchors and chemical bonding area at the CFRTP-metal interface as the result of porous metal surface filled with plastics.
3. The strength of the laser processed Al alloy-CFRTP joint reduced largely with the depth and width of the laser processed beads, which was mainly caused by the increase of bubbles near the interface.

CRediT authorship contribution statement

L.H. Wu: Writing - original draft, Writing - review & editing.

Declarations of Competing Interest

None.

Acknowledgement

This work is partly supported by the National Natural Science Foundation of China under Grant No. 51975553 and the IMR SYNL-T.S. Kê Research Fellowship. The authors gratefully thank Mr. M. Itakura and Mr. S. Shibata, Daicel Polymer Ltd., for the laser processing pretreatment of metal surfaces. The author L.H. Wu gratefully acknowledges Mr. B. Chen for the experimental help.

Data availability statement

The raw/processed data required to reproduce these findings cannot be shared at this time as the data also forms part of an ongoing study.

Appendix A. Supplementary data

Supplementary data to this article can be found online at https://doi.org/10.1016/j.compstruct.2020.112167.

References

[1] Goushegir SM, dos Santos JF, Amancio-Filho ST. Failure and fracture micro-mechanisms in metal-composite single lap joints produced by welding-based joining techniques. Compos A 2016;81:121–8.
[2] Goushegir SM, dos Santos JF, Amancio ST. Friction Spot Joining of aluminum AA2024/carbon-fiber reinforced poly(phenylene sulfide) composite single lap joints: Microstructure and mechanical performance. Mater Des 2014;54:196–206.
[3] Goushegir SM, dos Santos JF, Amancio ST. Influence of process parameters on mechanical performance and bonding area of AA2024/carbon-fiber-reinforced poly (phenylene sulfide) friction spot single lap joints. Mater Des 2015;83:431–42.
[4] Kolesnikov B, Herbeck L, Fink A. CFRP/titanium hybrid material for improving composite bolted joints. Compos Struct 2008;83:368–80.
[5] Camanho PP, Fink A, Obst A, Pimenta S. Hybrid titanium-CFRP laminates for high-performance bolted joints. Compos A 2009;40:1826–37.
[6] Kwon DS, Yoon SH, Hwang HY. Effects of residual oils on the adhesion characteristics of metal-CFRP adhesive joints. Compos Struct 2019;207:240–54.
[7] Katayama S, Kawahito Y. Laser direct joining of metal and plastic. Scr Mater 2008;59:1247–50.
[8] Zhang Z, Shan J-G, Tan X-H, Zhang J. Effect of anodizing pretreatment on laser joining CFRP to aluminum alloy A6061. Int J Adhes Adhes 2016;70:142–51.
[9] Zhang Z, Shan J, Tan X. Evaluation of the CFRP grafting and its influence on the laser joining CFRP to aluminum alloy. J Adhes Sci Technol 2018;32:390–406.
[10] Tan X, Zhang J, Shan J, Yang S, Ren J. Characteristics and formation mechanism of porosities in CFRP during laser joining of CFRP and steel. Compos B 2015;70:35–43.
[11] Jung KW, Kawahito Y, Katayama S. Laser direct joining of carbon fibre reinforced plastic to stainless steel. Sci Technol Weld Joining 2011;16:676–80.
[12] Balle F, Wagner G, Eifler D. Ultrasonic metal welding of aluminium sheets to carbon fibre reinforced thermoplastic composites. Adv Eng Mater 2009;11:35–9.
[13] Wagner G, Balle F, Eifler D. Ultrasonic welding of aluminum alloys to fiber reinforced polymers. Adv Eng Mater 2013;15:792–803.
[14] Balle F, Emrich S, Wagner G, Eifler D, Brodyanski A, Kopnarski M. Improvement of ultrasonically welded aluminum/carbon fiber reinforced polymer-joints by surface technology and high resolution analysis. Adv Eng Mater 2013;15:814–20.
[15] Wu LH, Wang D, Xiao BL, Ma ZY. Microstructural evolution of the thermo-mechanically affected zone in a Ti-6Al-4V friction stir welded joint. Scr Mater 2014;78–79:17–20.
[16] Wu LH, Hu XB, Zhang XX, Li YZ, Ma ZY, Ma XL, et al. Fabrication of high-quality Ti joint with ultrafine grains using submerged friction stirring technology and its microstructural evolution mechanism. Acta Mater 2019;166:371–85.
[17] Commin L, Dumont M, Masse JE, Barrallier L. Friction stir welding of AZ31 magnesium alloy rolled sheets: influence of processing parameters. Acta Mater 2009;57:326–34.
[18] Wu LH, Zhang H, Zeng XH, Xue P, Xiao BL, Ma ZY. Achieving superior low temperature and high strain rate superplasticity in submerged friction stir welded Ti-6Al-4V alloy. Sci China Mater 2018;61:417–23.
[19] Khan NZ, Siddiquee AN, Khan ZA, Mukhopadhyay AK. Mechanical and microstructural behavior of friction stir welded similar and dissimilar sheets of AA2219 and AA7475 aluminium alloys. J Alloy Compd 2017;695:2902–8.
[20] Wu LH, Nagatsuka K, Nakata K. Direct joining of oxygen-free copper and carbon-fiber-reinforced plastic by friction lap joining. J Mater Sci Technol 2018;34:192–7.
[21] Wu LH, Nagatsuka K, Nakata K. Achieving superior mechanical properties in friction lap joints of copper to carbon-fiber-reinforced plastic by tool offsetting. J Mater Sci Technol 2018;34:1628–37.
[22] Liu FC, Liao J, Nakata K. Joining of metal to plastic using friction lap welding. Mater Des 2014;54:236–44.
[23] Nagatsuka K, Yoshida S, Tsuchiya A, Nakata K. Direct joining of carbon-fiber-reinforced plastic to an aluminum alloy using friction lap joining. Compos B 2015;73:82–8.
[24] Amancio-Filho ST, Bueno C, dos Santos JF, Huber N, Hage Jr. E. On the feasibility of friction spot joining in magnesium/fiber-reinforced polymer composite hybrid structures. Mater Sci Eng A 2011;528:3841–8.
[25] Nagatsuka K, Kitagawa D, Yamaoka H, Nakata K. Friction Spot Joining of aluminum AA2024/carbon-fiber reinforced poly(phenylene sulfide) composite single lap joints: Microstr. mech. perform. ISIJ Int 2016;56:1226–31.
[26] Amend P, Pfindel S, Schmidt M. Thermal joining of thermoplastic metal hybrids by means of mono- and polychromatic radiation. Phys Proc 2013;41:98–105.
[27] Liu FC, Liao J, Gao Y, Nakata K. Effect of plasma electrolytic oxidation coating on joining metal to plastic. Sci Technol Weld Join 2015;20:291–6.
[28] Huang Y, Meng X, Wang Y, Xie Y, Zhou L. Joining of aluminum alloy and polymer via friction stir lap welding. J Mater Process Technol 2018;257:148–54.
[29] Huang Y, Meng X, Xie Y, Li J, Wan L. Joining of carbon fiber reinforced thermoplastic and metal via friction stir welding with co-controlling shape and performance. Compos A 2018;112:328–36.
[30] Miwa T, Kitagawa D, Nagatsuka K, Yamaoka H, Ito K, Nakata K. Dissimilar materials joining between stainless steel and carbon fiber reinforced thermoplastic by friciton lap joining. Q J Jpn Weld Soc (Japanese) 2017;35(1):29–35.
[31] Pabandi HK, Movahedi M, Kokabi AH. A new refill friction spot welding process for aluminum/polymer composite hybrid structures. Compos Struct 2017;174:59–69.
[32] Lambiase F, Paoletti A, Grossi V, Ilio AD. Friction assisted joining of aluminum and PVC sheets. J Manuf Proc 2017;29:221–31.
[33] Lambiase F, Paoletti A. Mechanical behavior of AA5053/polyetheretherketone (PEEK) made by friction assisted joining. Compos Struct 2018;189:70–8.
[34] Lambiase F, Paoletti A. Friction assisted joining of titanium and polyetheretherketone (PEEK) sheets. Thin-Walled Struct 2018;130:254–61.
[35] Kitagawa D, Nagatsuka K, Nakata K. Direct joining of plastics to carbon steel by friction lap joining. Proceedings of the 1st International Joint Symposium on Joining and Welding. 2013. p. 111–4.
[36] Nagatsuka K, Tanaka H, Xiao BL, Tsuchiya A, Nakata K. Effect of silane coupling treatment on the joint characteristics of friction lap joined Al alloy/CFRP. Q J Jpn Weld Soc (Japanese) 2015;33:317–25.
[37] Nagatsuka K, Xiao BL, Tsuchiya A, Tsukamoto M, Nakata K. Dissimilar materials joining of Al alloy/CFRTP by friction lap joining. Trans JWRI 2015;44:9–14.
[38] Liu FC, Dong P, Lu W, Sun K. On formation of Al-O-C bonds at aluminum/polyamide joint interface. Appl Surf Sci 2019;466:202–9.
[39] Esteves JV, Goushegir SM, dos Santos JF, Canto LB, Hage Jr. E, Amancio-Filho ST. Friction spot joining of aluminum AA6181-T4 and carbon fiber-reinforced poly (phenylene sulfide): effects of process parameters on the microstructure and mechanical strength. Mater Des 2015;66:437–45.
[40] Andre NM, Goushegir SM, dos Santos JF, Canto LB, Amancio-Filho ST. Friction Spot Joining of aluminum alloy 2024–T3 and carbon-fiber-reinforced poly(phenylene sulfide) laminate with additional PPS film interlayer: microstructure, mechanical strength and failure mechanisms. Compos B 2016;94:197–208.
[41] Han SC, Wu LH, Jiang CY, Li N, Jia CL, Xue P, et al. Achieving a strong polypropylene/aluminum alloy friction spot joint via a surface laser processing pretreatment. J Mater Sci Technol 2020. https://doi.org/10.1016/j.jmst.2020.02.035.